Available online at www.sciencedirect.com

ScienceDirect

Ceramics International 41 (2015) 13012–13024

CERAMICS INTERNATIONAL

www.elsevier.com/locate/ceramint

Mechanical and durability properties of alkali-activated mortar based on sugarcane bagasse ash and blast furnace slag

Adriana Pereira[a], Jorge L. Akasaki[a], José L.P. Melges[a], Mauro M. Tashima[a,*], Lourdes Soriano[b], María V. Borrachero[b], José Monzó[b], Jordi Payá[b]

[a]UNESP–Univ Estadual Paulista, Campus de Ilha Solteira, Alameda Bahia 550, Ilha Solteira, SP CEP 15385-000, Brazil
[b]Instituto de Ciencia y Tecnología del Hormigón, Universitat Politècnica de València, Camino de Vera s/n, Edificio 4G, Valencia 46022, Spain

Received 24 February 2015; received in revised form 23 June 2015; accepted 1 July 2015
Available online 8 July 2015

Abstract

Sugarcane bagasse is an agricultural waste which can be transformed, for cementing purposes, into an interesting material by combustion. Specifically, the ash (SBA) obtained by auto-combustion was used for preparing alkali-activated cements by blending blast furnace slag (BFS). SBA had a large amount of quartz; however, it reacted in high alkaline medium. Mixtures of BFS/SBA have been used for preparing alkali-activated mortars, by using NaOH (8 M solution), sodium silicate (8 M solution in Na^+ and SiO_2/Na_2O molar ratio of 0.5) and KOH (8 M solution) as activating solutions. Replacements of 25%, 33% and 50% of BFS by SBA were carried out and compressive strengths in the range 16–51 MPa were obtained after 90 curing days. Microstructural studies demonstrated that the hydration products formed in the activation of BFS are not significantly affected by the presence of SBA in the mixture. The durability of alkali-activated mortars was compared to ordinary Portland cement (OPC) mortar in the following media: hydrochloric acid, acetic acid, ammonium chloride, sodium sulphate and magnesium sulphate. The behaviour of alkali-activated mortars with BFS and BFS/SBA was better than that found for plain OPC mortars, especially in ammonium chloride, acetic acid and sodium sulphate media. After 200 days of testing in ammonium chloride solution, the compressive strength loss for Portland cement mortar was about 83.3%. For the same test conditions, alkali-activated mortars presented a maximum reduction of 48.4%. The presence of SBA in alkali-activated BFS mortars did not produce any serious problems in durability. As a general conclusion, sugarcane bagasse ash (SBA) obtained by auto-combustion showed good cementing properties as a mineral precursor blended with blast furnace slag (BFS) in alkali-activated systems.

Keywords: C. Strength; Alkali activation; Blast furnace slag; Sugarcane bagasse ash; Durability

1. Introduction

The increase in the world's population associated with economic development is generating several problems that are contributing to the global climate change. In the last decades, the world energy supplies have been dominated by fossil fuel (approximately, 80%), which can be associated with environmental problems such as acid rain and greenhouse gas emissions. In the last years, renewable energy sources like wind, solar and biomass have been used in order to promote sustainable development.

Nowadays, biomass represents only about 9–14% of energy sources for industrialised countries and in developing countries, this value is about 20–33% [1]. It is important to state that the energy production from biomass can be considered a renewable energy and this process does not release new CO_2 into the atmosphere: the carbon dioxide is only cycled in the atmosphere.

In Brazil, especially in the São Paulo state, the main agroindustrial activity is associated with sugarcane production

*Corresponding author. Tel.: +55 1837431217.
E-mail addresses: adrianapereiradu@gmail.com (A. Pereira), akasaki@dec.feis.unesp.br (J.L. Akasaki), jlpmelges@dec.feis.unesp.br (J.L.P. Melges), maumitta@hotmail.com (M.M. Tashima), lousomar@upvnet.upv.es (L. Soriano), vborrachero@cst.upv.es (M.V. Borrachero), jmmonzo@cst.upv.es (J. Monzó), jjpaya@cst.upv.es (J. Payá).

http://dx.doi.org/10.1016/j.ceramint.2015.07.001
0272-8842/

(approximately, 500 Mt annually). At first, this activity was only associated with the extraction of sugar and ethanol. In the last years, the sugarcane industry has been exploiting the use of sugarcane bagasse as biomass in the production of energy. From this process, about 3 Mt of sugarcane bagasse ash (SBA) is being generated annually.

The main use for this waste material is as a supplementary cementitious material (SCM) in the production of cement, concretes and mortars based on Portland cement [2–5]. According to Fairbairn et al. [2], SBA is an active pozzolanic material which can replace partially the clinker in the cement production significantly reducing the CO_2 emissions into the atmosphere (estimated reduction is about 519.3 kt of CO_2 per year).

Frías et al. [3] assessed the use of three different SBA from the same bagasse waste generated in a sugar factory. The morphology and the pozzolanic reactivity, determined though the fixed lime, of SBA are directly related to the burning temperature of bagasse. In the same way, Cordeiro et al. [4] studied the influence of calcination temperature on the pozzolanic activity of sugarcane bagasse ash. Sugarcane was pre-calcined at 350 °C for three hours and then calcined at 400–800 °C for another three hours. Depending on the calcination temperature, the pozzolanic activity index of SBA was in the range 28–77%.

Nevertheless, it is important to note that the use of SBA as a pozzolanic material is limited to the range 10–35% of Portland cement replacement. Due to this limitation, and thinking about the sustainable development that the reduction on the Portland cement consumption can generate, several studies have been performed in order to produce alternative binders that reduce the raw material and energy consumption and, consequently, the environmental problems associated with the Portland cement production.

The production of alternative binders from the alkaline activation of aluminosilicate materials, the so called alkali-activated binders, is a very interesting alternative for reducing the raw materials consumption and the CO_2 emissions [6]. In the last 20 years, there has been an exponential increase in the number of reports, papers and books related to this issue [7]. Alkali-activated binders are cementitious materials formed by a chemical reaction of an alkaline solution and an amorphous aluminosilicate material that forms materials with binding properties. Usually, alkali-activated binders are produced using fly ash, metakaolin or blast furnace slag as aluminosilicate material [8]. However, as mentioned by Payá et al. [9] in the Handbook of Alkali-Activated Cements, Mortars and Concretes, the development of new precursors is necessary in order to propose this type of binder as cement for the future. Lancellotti et al. [10] assessed the use of incinerator bottom ash in the production of alkali-activated binders using alkaline solutions of concentrated NaOH and waterglass solutions.

In the same way, Payá et al. [9] presented several waste materials that have been investigated in the production of alkali-activated binders, including the use of SBA, in chapter 18 of that book. All of these waste materials can present high degree of valorisation if they are well used for a fixed purpose.

The production of alkali-activated binders is limited to the availability of mineral precursors. In some developing countries it could be interesting to combine selected ashes from agrowastes with typical precursors such as blast furnace slag or fly ash. Sugarcane bagasse ash is one of these options and, it application success will depend on the combustion conditions of sugarcane bagasse, it means, on the physical and chemical properties of SBA.

Castaldelli et al. [11] studied the use of SBA generated in a sugar factory for preparing alkali-activated systems based on binary systems of blast furnace slag (BFS)/SBA. According to the authors, even presenting a high proportion of organic matter (about 25%) and high percentage of impurities (calcite and quartz), SBA from a sugar factory can be an interesting material for producing alkali-activated binders. Mortars cured at 65 °C for 3 and 7 days presented compressive strength values in the range 42.8–53.5 MPa, depending on the proportion of BFS/SCBA (85/15, 75/25 and 60/40). In the same way, mortars cured at room temperature for long curing times presented higher compressive strength than mortars cured at 65 °C and the total porosity of these mortars was also reduced [11]. Recently, Castaldelli et al. [12] presented another paper where the use of fly ash/SBA was reported. In this study, authors calcinated (650 °C during 2 h) the SBA from sugar factory in order to reduce the amount of organic matter and carbon, and using this procedure, it was possible to obtain alkali-activated mortars with good performance.

Moreover, the detailed chemical understanding and the durability properties of these alternative binders are the other main parameters that enable the commercialisation process of alkali-activated binders [13]. In the last years, several papers have reported the durability aspects of alkali-activated binders [14–15]. In general terms, the lower the permeability of concrete, the greater the resistance of concrete to external attacks. Comparing to OPC binders, alkali-activated materials present greater resistance to acidic attack due higher alkalinity of the pore and lower CaO/SiO_2 ratio in the alkali-activated systems [16]. Sulphates attack on alkali-activated binders depends on factors such as the type of activating solution, concentration of alkaline solution and type of cation in the sulphate medium [17–18].

In this paper, studies on reactivity of SBA obtained from auto-combustion conditions are carried out. The valorisation of these ashes in alkali-activated mixtures using blast furnace slag (BFS) is proposed. Selected mixtures replacing part of BFS by SBA obtained by auto-combustion were assessed when sodium hydroxide, sodium silicate and potassium hydroxide solutions were used as activating solutions. In the same way, for selected specimens, durability studies were performed by means of acid attack (hydrochloric acid, acetic acid and ammonium chloride) and sulphate attack (sodium and magnesium sulphates).

2. Experimental section

2.1. Preparation of sugarcane bagasse ash (SBA)

SBA was prepared by auto-combustion [19] of sugarcane bagasse obtained from a sugar industry in Brazil. The process takes 12–14 h for burning 10 kg of biomass. The collected ashes were sieved (2.38 mm) for removing unburned pieces of bagasse. The sieved sample was ground to reduce its fineness.

Table 1
Chemical composition of SBA, BFS and OPC (% by weight).

Parameter	BFS	SBA	OPC
SiO_2	32.96	78.59	18.16
Al_2O_3	11.51	4.47	7.01
Fe_2O_3	0.56	4.88	2.57
CaO	43.54	1.34	62.95
Na_2O	0.35	0.22	0.18
K_2O	0.41	2.37	0.77
SO_3	1.89	0.66	3.11
Cl	0.10	0.13	0.02
MgO	7.32	1.03	0.50
TiO_2	0.50	1.16	0.10
Others	0.76	0.74	0.48
LOI	0.10	4.40	4.07

2.2. Materials

Blast furnace slag was supplied by a Brazilian producer (Rio Pardo Tratamento de Resíduos Industriais Ltda – Ribas do Rio Pardo/MS). It had an appropriate fineness for research purposes (mean particle diameter = 27.50 μm; $d(0,1) = 4.21$ μm; $d(0,5) = 21.43$ μm; $d(0,9) = 58.56$ μm). Brazilian Portland cement CP V ARI HOLCIM was used for preparing OPC control mortars studied in Section 3.4. Its chemical composition is given in Table 1. This cement fulfils the Brazilian standard NBR 5733 [20]. Natural sand was used for preparing mortars, and it fulfils the requirements according to Brazilian standards NBR 248 [21] and NBR 52 [22]. It had 2.61 specific gravity and 2.03 fineness modulus.

Chemical reagents were supplied by Dinâmica Química Contenporânea (São Paulo, Brazil). Sodium hydroxide and potassium hydroxide had a purity of 97% and 85%, respectively. Sodium silicate was supplied as a white powder, with the following composition: 18% Na_2O and 63% SiO_2. Sodium sulphate (> 99% purity), magnesium sulphate (> 99% purity), hydrochloric acid (37% purity), acetic acid (99.7% purity) and ammonium chloride (99.5% purity) were used to prepare aggressive solutions for durability studies.

2.3. Techniques and procedures

A ball mill composed of 684 steel cylinders whose total weight was about 52.5 kg was used for SBA grinding. Here, 5 kg of the material (unground SBA) was placed and milled for a period of 50 min. Sample collections were carried out every 5 min in order to perform analysis of the evolution of particle sizes over the 50 min (determined by laser diffraction in a Mastersizer 2000, Malvern Instruments). The chemical composition of SBA, BFS and OPC was determined by X-ray fluorescence (XRF, Philips Magix Pro). The Fourier-transformed infrared spectroscopy (FTIR, Bruker Tensor 27 Platinum ATR spectrometer) data were collected in the transmittance mode, from 4000 to 400 cm^{-1}. A TGA 850 Mettler-Toledo thermobalance was used, which allows the measurement of thermogravimetric curve and differential thermal analysis curve simultaneously. Then, 70 μL alumina crucibles were used for heating in the range 35–1000 °C (75 mL min^{-1} of air gas flow, heating rate of 20 °C min^{-1}) and sealed 100 μL aluminium crucibles with a pin-holed lid were used for heating range 35–600 °C (75 mL min^{-1} of nitrogen gas flow, heating rate of 10 °C min^{-1}). Scanning electron microscopy (SEM) studies were carried out in a JEOL JSM-6300: samples were covered with gold. The mercury intrusion porosimetry (MIP) was performed on a porosimeter AutoPore IV 9500 of Micrometrics Instrument Corporation with a range of pressures between 13.782 Pa and 227.4 MPa. Mortar samples were evaluated at a pressure up to 0.21 MPa in the low pressure port, and at 227.4 MPa in the high pressure port. After mercury intrusion, the extrusion process was also monitored.

Preparation of activating solutions: NaOH and KOH solutions were prepared dissolving the solid reagent in the corresponding amount of water for preparing 8 M solutions in Na^+ or K^+ ions. Sodium silicate (SS) solution was prepared by dissolving the corresponding amount of solid NaOH in water, and while hot, solid sodium silicate reagent was added. The mixture was stirred for complete dissolution and then cooling at room temperature.

Preparation of paste samples: both solids, BFS and SBA, were mixed in dry state, and then the activating solution was added. The fresh paste was hand-mixed for 5 min and then stored in a sealed plastic container. The containers were stored at 25 °C until the testing age.

Preparation of mortar samples: both solids, BFS and SBA, were hand mixed in dry state and then added to the activating solution. The mixture was stirred at low speed (124 rpm) for 30 s and at medium speed (220 rpm) for 30 s; then sand was added while stirring for the next 60 s at low speed; the mixture was stirred for 30 s at medium speed and 30 s at high speed (450 rpm). The stirring was stopped for 60 s and finally the mixture was stirred for an additional 60 s at medium speed. Cubic ($5 \times 5 \times 5$ cm^3) moulds were filled and compacted (vibration table) with fresh mortar, and cured in a humid chamber at 25 °C. Specimens were demoulded after 24 h, covered with plastic film and stored in the same chamber until testing age. Portland cement mortars were produced according to Brazilian standard NBR 7215 [23]. The water absorption in mortars was carried out according to Brazilian standard NBR 9778 [24].

Preparation of solutions for durability studies: aggressive solutions were prepared by dissolving commercial products in deionised water. Acid solutions had the following concentrations: hydrochloric acid (HCl, 0.5 M), acetic acid (HAc, 1 M) and ammonium chloride (NH_4Cl, 1 M). Sodium sulphate (Na_2SO_4) was prepared in 10% and magnesium sulphate ($MgSO_4$) in 5% by weight of deionised water.

2.4. Notation of samples

Three sets of samples were established: NaOH-set, KOH-set and SS-set, depending on the activating solution used. The notation for pastes and mortars was as follows: AA-*XX*%, with AA being the type of activating solution (NaOH, KOH, SS) and *XX* representing the replacing percentage of slag by SBA (00%, 25%, 33% and 50%).

3. Results and discussion

3.1. Characterisation of sugarcane bagasse ash (SBA)

Chemical compositions for SBA and blast furnace slag (BFS) are summarised in Table 1. SBA presented SiO_2 as the main oxide (78.59%). The sum of acid oxides (oxides of Si, Al and Fe) was 87.94%. Taking into account this percentage of oxides, and based on previous papers [25–26], SBA could be used as mineral matter for alkaline activation. SBA was rich in alkalis, specifically in potassium (2.37%), which was typically found for ashes obtained from biomass.

XRD pattern showed the presence of quartz (PDF Card 331161), with no deviation in the baseline observed (See Fig. 1). This means that an important fraction of the ash is crystalline matter, and the quartz probably appeared because of contamination of the bagasse with soil. During the collection in the field, part of the soil is mixed with the sugarcane pieces and then, finally, they are deposited together with the bagasse after the extraction of sugar. BFS presented the typical amorphous structure, as can be seen in Fig. 1. The insoluble residue (IR) for SBA was calculated, in term of assessing the fraction of ash that could give reactivity in alkaline medium. The IR for SBA was 75.0%, meaning that a large part of the ash particles will not dissolve in alkaline solution. Certainly, the most important part of the insoluble residue was related to the quartz identified by XRD. This fact could limit the reactivity of SBA in alkali-activated binders.

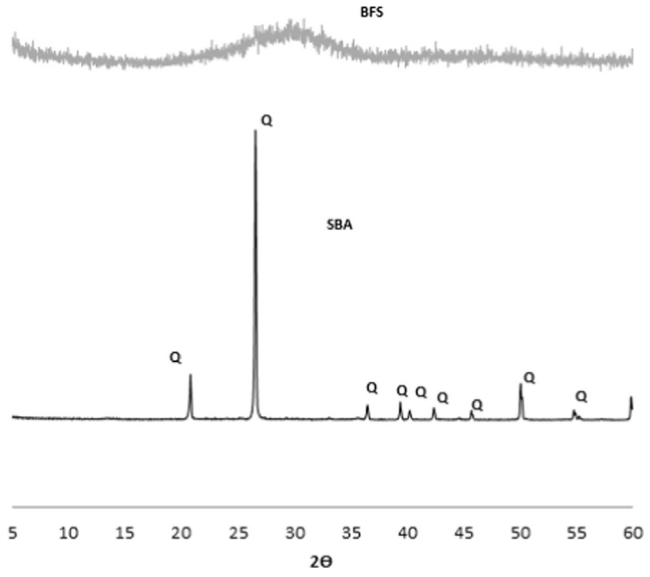

Fig. 1. X-ray diffractogramms for SBA and BFS (Key: Q=Quartz).

As can be seen in Table 1, the loss on ignition was only 4.40% for SBA, which means that the auto-combustion process was very effective. The volatilised matter when firing was organic matter and/or carbon, as can be seen (Fig. 2) in the thermogravimetric curve (TG), its derivative curve (DTG) and the differential thermal analysis curve (DTA, Fig. 2b). The sample was monitored in a thermobalance for the temperature range of 100–1000 °C in a dried air atmosphere, using a heating rate of 20 °C min^{-1} and an alumina crucible. The most important mass loss was found in the 350–550 °C range, which is attributed to organic matter. Two peaks at 417 °C and 497 °C were observed in the DTG curve, due to a different oxidation/volatilisation processes. Also, a small peak at a higher temperature (671 °C) was due to decomposition of some carbonates. In the DTA curve (Fig. 2b), two exothermic peaks were observed at 438 °C and 502 °C, which are related to the mass loss peaks in the DTG curve for oxidation/volatilisation of organic matter.

The fineness of SBA was assessed. After auto-combustion, the ash was collected and then sieved for removing unburned particles. Thus, the ash particles were too large for cementing purposes, and consequently had to be ground. The grinding was carried out for 50 min, and samples were taken every five minutes to assess the effectiveness of the grinding process. Table 2 summarises the main granulometric parameters for ground samples. In the first five minutes of grinding, the mean particle size was 87.9 μm. This value was reduced by 50% after a further 30 min of grinding. However, to increase reactivity, a total time of 50 min was selected to yield a mean particle diameter lower than 35 μm. This sample showed 50% of the volume less than 25.1 μm and 90% less than 82.3 μm. The ground SBA was slightly coarser than BFS, which had a

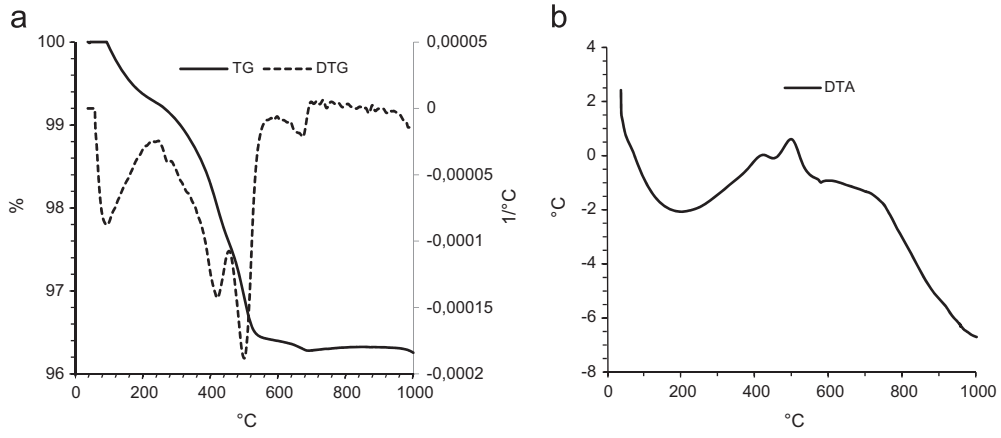

Fig. 2. Thermal analysis: (a) TG and DTG curves; (b) DTA curves for SBA (heating in dried air).

mean particle diameter of 27.50 μm and 50% of the volume was less than 21.43 μm.

SBA particles were irregular in shape, as can be seen in Fig. 3. Larger particles were denser, probably due to the presence of quartz (this was tested by means EDX technique). Smaller particles presented rough surfaces, a behaviour attributed to the elimination of organic matter from bagasse, leaving the inorganic fraction (rich in silicon and potassium). Spherical-shaped particles were not found, suggesting that the combustion temperature reached in the burning process did not produce the melting of inorganic matter.

3.2. Mechanical strength studies

Alkali-activated (AA) cements were prepared using blast furnace slag (control BSF mortars) or a mixture of BFS and SBA (the content of these both materials is considered as the binder). In Table 3, the composition of the prepared mortar is summarised. For all mortars, the water/binder ratio was 0.45, except for the KOH series ($w/b = 0.40$). According to Tashima [27], the use of KOH solutions allows a reduction in the w/b ratio when compared to NaOH solutions. Also, for all mortar, the aggregate/binder ratio was 2.5. Three different sets of mortars were prepared. The first (NaOH-set) corresponds to the use of NaOH solution (8 mol L^{-1}); for this set, the replacement of slag by SBA was carried out by mass in 25%, 33% and 50%. For the second set of mortars (SS-set), a sodium silicate solution was used, which was prepared by mixing NaOH and solid sodium silicate in water. For this solution, 8 mol L^{-1} of sodium cation (Na^+) was prepared and the SiO_2/Na_2O molar ratio (ε) was kept in 0.5. Also, for this set, replacements of 25%, 33% and 50% of slag by SBA were carried out. Finally, for the third set (KOH-set), 8 mol L^{-1} solution of KOH was used as the alkaline activator. In this case, only control mortar containing slag and mortar with 25% replacement by SBA were prepared.

Prepared mortars were stored in a humid chamber at 25 °C until mechanical testing age. Mortars were tested after 3, 7, 14, 28 and 90 days of curing. Only for NaOH-set mortars with 33% and 50% replacements was a thermal activation of fresh mixtures required for the first step of curing: these mixtures did not set after 24 h of curing at 25 °C, and after this period a thermal curing step at 65 °C for 7 h was required for hardening. In Table 4, compressive strength values for all of the prepared mortars are summarised.

Table 2
Mean particle diameter, $d(0,1)$, $d(0,5)$ and $d(0,9)$ for different grinding time samples for SBA and for as-received BFS.

Grinding time (min)	$d(0,1)$ (μm)	$d(0,5)$ (μm)	$d(0,9)$ (μm)	Mean particle diameter (μm)
05	4.0	52.4	202.8	87.9
10	3.5	48.4	162.8	69.2
15	3.3	44.3	136.6	58.2
20	3.1	40.0	125.3	53.4
25	2.9	35.1	115.8	48.6
30	2.4	33.4	106.4	45.0
35	2.6	31.5	99.5	42.3
40	2.5	28.0	93.0	39.1
45	2.2	28.2	90.0	38.3
50	2.2	25.1	82.3	34.6
BFS	4.2	21.4	58.6	27.5

Table 3
Composition of prepared mortars. ($[M^+]$: concentration of alkaline element (Na^+ or K^+) in the activation solution; ε: SiO_2/Na_2O molar ratio).

Mortars	Solution	$[M^+]$ (mol L^{-1})	ε	%SBA	%BFS
NaOH-00%	NaOH	8	0	0	100
NaOH-25%			0	25	75
NaOH-33%			0	33	67
NaOH-50%			0	50	50
KOH-00%	KOH	8	0	0	100
KOH-25%			0	25	75
SS-00%	NaOH + SS	8	0.5	0	100
SS-25%			0.5	25	75
SS-33%			0.5	33	67
SS-50%			0.5	50	50

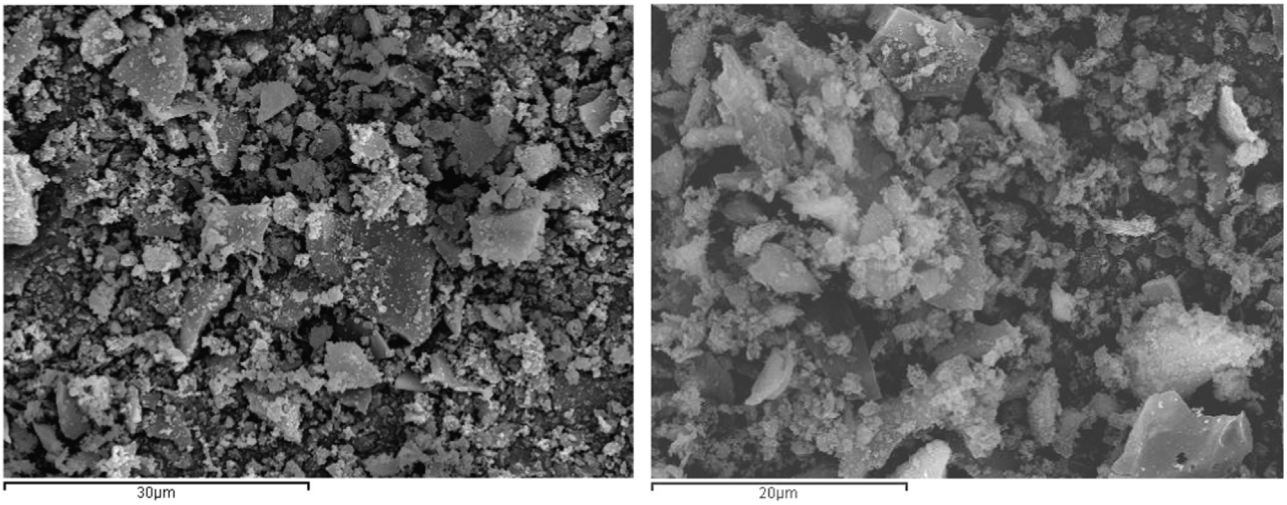

Fig. 3. Scanning electron microscopy micrographs of SBA.

Table 4
Mechanical compressive strengths (MPa) for prepared mortars.

Curing time					
Mortars	3 days	7 days	14 days	28 days	90 days
NaOH-00%	5.5 ± 0.1	10.4 ± 0.5	15.5 ± 0.8	21.4 ± 2.4	26.3 ± 1.6
NaOH-25%	3.8 ± 0.1	12.7 ± 0.8	19.7 ± 0.4	25.0 ± 0.6	27.4 ± 1.4
NaOH-33%*	9.0 ± 0.2	9.2 ± 0.1	10.7 ± 0.4	16.3 ± 0.7	20.8 ± 0.2
NaOH-50%*	5.1 ± 0.1	6.6 ± 0.2	8.0 ± 0.1	12.6 ± 0.7	16.1 ± 1.5
SS-00%	7.1 ± 0.1	16.2 ± 0.4	27.5 ± 0.8	30.4 ± 1.8	38.9 ± 1.5
SS-25%	2.9 ± 0.1	10.9 ± 0.3	19.3 ± 0.7	39.5 ± 3.6	42.1 ± 2.9
SS-33%	2.5 ± 0.2	13.2 ± 0.4	16.4 ± 1.0	23.7 ± 0.8	30.3 ± 1.2
SS-50%	3.7 ± 0.9	6.3 ± 1.3	13.5 ± 1.3	18.0 ± 1.5	26.4 ± 1.6
KOH-00%	5.7 ± 0.2	18.0 ± 0.4	32.0 ± 1.3	35.5 ± 3.2	46.2 ± 0.7
KOH-25%	4.0 ± 0.1	14.0 ± 0.4	31.3 ± 1.4	35.0 ± 2.9	51.3 ± 1.2

*Previous thermal activation: 7 h at 65 °C.

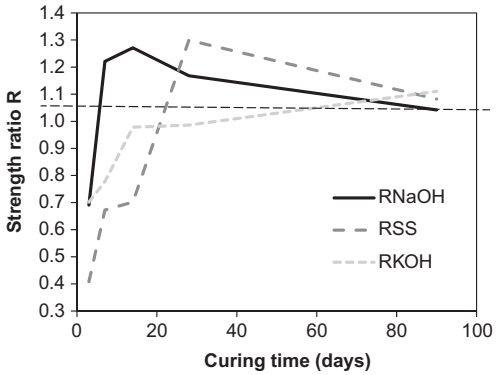

Fig. 4. Strength ratio (R) between 25% BSA containing mortars and the corresponding 0% SBA mortars for different curing times and different alkaline activating solutions (NaOH, SS and KOH).

Control mortar prepared by activation of slag by NaOH solution (NaOH-00%) showed increasing compressive strength behaviour in the 3–90 day period. Compressive strength of NaOH-0% mortar after 28 days was 21.4 MPa. This value was similar when compared to those found for several authors [28–30]. The replacement of slag by SBA by 25% produced a decrease in compressive strength for the shortest curing time, suggesting that the contribution of SBA to the development of hardened matrix was negligible. Interestingly, for longer curing times, the contribution of SBA to the development of compressive strength was noticeable. Thus, after 28 days of curing, compressive strength for NaOH-25% was 3.6 MPa higher than NaOH-00%. When the replacing percentage was increased to 33% and 50%, the initial hardening process was seriously modified, and an additional thermal curing was required. In this way, interesting compressive strength values were reached after 3 days of age. The development of strength was similar to NaOH-00% and NaOH-25% mortars; however, for NaOH-33% and NaOH-50%, the maximum values after 90 days of curing were 20.8 and 16.1 MPa, respectively, both values significantly lower than those obtained for NaOH-00% and NaOH-25%. This means that the reduction of slag content was not compensated by the presence of SBA in terms of developed strength for the studied curing period. The behaviour of NaOH-25% mixture at 90 days of curing is noticeable, for which 27.4 MPa was obtained: in this case, SBA and slag were equivalent in terms of strength, suggesting that SBA is reactive in this mixture and contributed in the same way as slag to the development of strength. In Fig. 4, the strength ratio of NaOH-25%/NaOH-00% (R_{NaOH}) is depicted, and it is noticeable the contribution of SBA because after 3 days of curing, the R_{NaOH} ratio was higher than the unit.

For SS-set, the behaviour of control mortar (SS-00%) was better in terms of strength development when compared to the NaOH-set. Thus, after 3 days, the compressive strength was increased to 7.1 MPa, and after 28 days it was 30.4 MPa (vs. 21.4 MPa for NaOH-set). These values were lower than those found for other authors [30], probably due to ε value for mortars tested in this research being too low. It is very interesting to note that the behaviour of SS-25% samples was also better than those found for SS-0% after 28 days of curing. However, the strength development for SS-25% was slower compared to the control sample SS-00%, suggesting that the contribution of SBA in the matrix took place longer-term. In this way, after 90 days of curing, the contribution of SBA to the system was very important and the yielded strength was higher than 40 MPa, indicating that the effect of SBA in the developed matrix was equivalent to those produced by slag. In Fig. 4, strength ratios SS-25%/SS-00% (R_{SS}) for the curing period studied are depicted, and it is noticeable in this case that R_{SS} values were higher than the unit after 14 days of curing, which was a longer period of time than that found for R_{NaOH}. This behaviour means that contribution to the strength of SBA, in the presence of sodium silicate as the activating solution, was delayed and thus the reactive silica in SBA reacted to a longer curing time.

For samples of SS-set with 33% and 50% replacements, no thermal activation of mortars was necessary, suggesting that the presence of silicate in the activating solution compensated the deleterious effect of the high replacement rate. Good strength evolutions were observed for these systems; however, strengths reached after 90 days were lower than those found for SS-00% (30.3 and 26.4 MPa for SS-33% and SS-50%, respectively, versus 38.9 MPa for control mortar), indicating again that the reactivity of SBA in these systems did not compensate the reduction in the slag content. This behaviour, together with that found for NaOH-set, demonstrated that the reactivity of SBA is very limiting, due to the high amount of quartz, which did not react in the studied conditions.

For KOH-set, the water/binder ratio was lower than those used for previous sets: 0.4 vs 0.45. The strength for control mortar KOH-00% was better than the corresponding NaOH-00%: thus, 35.5 MPa was reached for KOH activated samples after 28 days of curing, with this value being higher than the corresponding value for the NaOH-00% sample (21.4 MPa). This enhancement is attributed to the reduction in the water/binder ratio and also to the better strength development for KOH activated systems [31]. The replacement of slag by SBA produced mortars with similar strengths to those found for KOH-00% after 28 days. In this case, the contribution of potassium to strength development in slag/SBA mixtures is lower with respect to that of sodium, because for 7 and 14 days

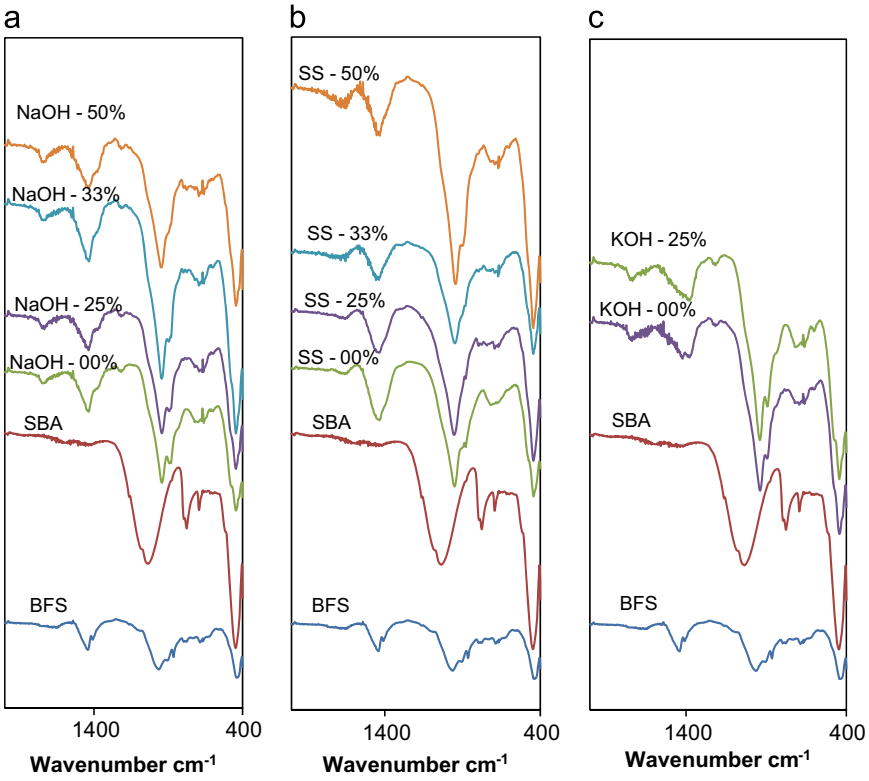

Fig. 5. FTIR spectra for pastes cured at 28 days: (a) NaOH-set; (b) SS-set; (c) KOH-set.

curing times, the strength ratio of KOH-25%/KOH-00% (R_{KOH}) was less than 1 (NaOH-25%/NaOH-00% ratio was higher than 1 for this 7–14 period as can be seen in Fig. 4). Finally, after 90 days of curing, the role of potassium in the development of strength was similar to that found for sodium, and the corresponding strength ratio R_{KOH} was equal to 1.11.

3.3. Microstructural studies

FTIR spectra for BFS and SBA are depicted in Fig. 5. The spectrum for BFS showed a broadband characteristic of gehlenite centred at 964 cm^{-1}, attributed to symmetric stretching vibration of Si(Al)–O–Si bonds. An intense peak attributed to carbonate anion vibration (ca. 1437 cm^{-1}) was also observed. In the spectrum for SBA, the highest intensity absorption peak was related to the Si(Al)–O–Si network: an intense a broadband centred at 1036 cm^{-1} (stretching vibration of Si–O–Si bonds). Also, peaks corresponding to quartz were noticed at 775 and 447 cm^{-1}. Additionally, a peak at 694 cm^{-1} was attributed to the presence of organic matter in the ash.

Pastes for the three sets of mixtures were characterised by means FTIR after 7, 28 and 90 days of curing. Fig. 5a shows the FTIR spectra for NaOH-set mixtures cured after 28 days. Similar FTIR spectra were obtained for the SS-set (Fig. 5b) and the KOH-set (Fig. 5c).

For the NaOH-set, the following points should be highlighted: for all pastes there is a broadband centred at 940–950 cm^{-1} range. A vibrational mode appeared in the 941–945 cm^{-1} range for 7-days pastes and it is assigned to the asymmetric stretching vibration of Si–O–T bonds, where T is tetrahedral silicon or aluminium [32]. A slight increase in wavenumber was observed after 28 days of curing (943–947 cm^{-1}) and at 90 days (945–949 cm^{-1}). This means that there is no important change in the nature of the hydrated compounds formed during the alkaline activation. Only a small difference was found for a vibration at 893 cm^{-1}, which appeared with more intensity for higher contents of BFS. In general, there was no significant difference when the ash replacement was increased. For the highest content of SBA (50% replacement) a shoulder to higher energy was observed for the peak centred at 940–950 cm^{-1}, which was attributed to the presence of more unreacted ash (which had a vibrational mode centred at 1036 cm^{-1}).

For the KOH-set, similar results were found: a broad peak centred at slightly lower energy than those found for the NaOH-set: 936 cm^{-1} after 7 days, 939 cm^{-1} for 28 days and 940 cm^{-1} for 90 days of curing. The same type of peak than NaOH-set at lower energies was observed (889–895 cm^{-1}).

Finally, for the SS-set, a slight shift for the main vibration band was observed: 951–954 cm^{-1} was the waveband range for this peak. The presence of sodium silicate in the activating solution produced more polymerisation of SiO_4 units. Only for SS-50% paste, was the vibration peak lower (945 cm^{-1}), probably due to the large percentage of unreacted SBA.

In general, the presence of SBA in the mixtures did not influence the nature of the hydrates formed during the alkaline activation process, yielding small differences when Na^+ was replaced by K^+ or when sodium silicate was added to the activating solution.

Pastes for the three sets of mixtures were also characterised by thermogravimetric (TG) analysis (7, 28 and 90 days of curing). The samples were taken and ground in acetone, and filtered and dried at 60 °C for 30 min. In all TG curves, an important mass loss was produced in the 100–250 °C range. DTG curves only showed a peak, which was centred in the 145–170 °C range. No additional peaks were observed at higher temperatures as previously reported for other slag [11]. Selected DTG curves for NaOH-set (0–50% replacement after 90 days of curing) are depicted in Fig. 6. In Table 5, total mass loss values (P_T) from TG curves and temperature peaks (T_{peak}) from the DTG curves are summarised. In general, the total mass loss increased for a given paste with curing time. Reached values after 90 days of curing were in the 12–14% range: this range is slightly lower than those found in the literature for similar blends and activating solutions [11] which suggests that the reactivity of the slag used in this work was lower. It is noticeable that the total mass loss values for SBA replaced pastes were similar to the corresponding control pastes, meaning that the presence of ash particles produced important quantities of hydrated compounds. This behaviour means that SBA is reactive in high alkalinity conditions, despite the presence of an important amount of quartz.

The mass loss observed was attributed to the decomposition/dehydration of gel formed in the alkaline activation of mineral matter. (C,N)–A–S–H gels released water when heated, and H_2O molecules bonded to gel and OH groups from the aluminosilicate network are volatilised.

DTG curves for pastes of KOH-set and SS-set were very similar to those found for NaOH-set pastes. For KOH-set pastes, the total mass loss (P_T) was slightly larger than for NaOH-set pastes, indicating that the gels formed have more combined water. The same occurred for SS-set pastes. Temperature peaks of the DTG curves were in the 151–169 °C range for KOH-set pastes and 145–156 °C range for SS-pastes. The replacement of BFA by SBA had no influence on the P_T and T_{peak} values.

Pastes (28 curing days) were characterised by the SEM–EDX technique. NaOH-00% and NaOH-25% were very similar in terms of the products formed. Only the presence of quartz particles in NaOH-25% pastes differentiated between them. In Fig. 7a, the microstructure of NaOH-25% is shown; three facts can be noticed: firstly (point A), the presence of a quartz particle; and secondly, the amorphous matrix (point B), which has the following molar ratios: Al/Si=0.32, Na/Si=1.34; Ca/Si=0.60 and K/Si=0.05. This (N,C)–A–S–H phase was very rich in sodium and calcium, and there is a small amount of potassium from the activated SCSA. Thirdly, a few crystals (probably zeolite, point C) were found, with the following relative chemical composition (molar ratio): Al/Si=0.63, Na/Si=0.63; Ca/Si=0.24 and K/Si=0.14. This type of crystal was also found in NaOH-33% and NaOH-50%, as can be seen in Fig. 7b. SS activated pastes did not present this type of crystal and an amorphous matrix was the most important phase (see Fig. 7c). This matrix had the following composition (point D): Al/Si=0.26, Na/Si=0.45; Ca/Si=1.28 and K/Si=0.07. Also, in these samples, some slag unreacted particles were found (point E, in Fig. 7c). More porous phases were found in these pastes (Fig. 7d), which presented similar chemical compositions to those mentioned above. Finally, micrographs for KOH-activated pastes are shown in Fig. 7e–h. A dense matrix was the most important phase (KOH-00%, see Fig. 7e, point F) and the chemical composition of the matrix included the following molar ratios: Al/Si=0.31, Ca/Si=0.81 and K/Si=0.76. Obviously, there is no of sodium in the matrix because the activator was potassium-based. Also in Fig. 7e (point G), an unreacted slag particle can be seen (chemical composition: Al/Si=0.30, Ca/Si=0.65 and K/Si=0.10). A few small cubic crystals (0.5–2 μm) were present in some parts of the matrix (Fig. 7f); these crystals (probably zeolites, point H) had the following composition: Al/Si=0.55, Ca/Si=0.46 and K/Si=0.64. The KOH-25% paste also presented the same type of cubic crystals (Fig. 7g) and a similar chemical composition. In this paste, some quartz particles appeared in the dense matrix (Fig. 7h, point I).

Durability properties for inorganic binders depend on, among others, the porosity and permeability of the matrix. It has been reported that significant differences in oxygen and chloride permeability have been observed when OPC mortars are compared to alkali-activated mortar prepared with natural

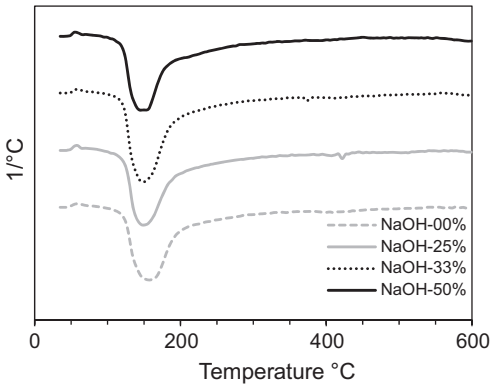

Fig. 6. DTG curves for NaOH-set pastes, with=0%, 25%, 33% and 50% replacement percentages of BFS by SBA.

Table 5
Total mass loss (P_T, %) in TG analysis for 35–600 °C temperature range and temperature peak (T_{peak}, °C) in the DTG curve for pastes.

Paste	P_T (%)	T_{peak} (°C)	P_T (%)	T_{peak} (°C)	P_T (%)	T_{peak} (°C)
	7 days		28 days		90 days	
NaOH-00%	7.3	157	8.7	158	12.5	157
NaOH-25%	9.9	162	9.5	150	12.5	148
NaOH-33%	9.7	155	9.5	151	13.6	150
NaOH-50%	7.0	161	9.0	151	12.4	145
KOH-00%	10.1	169	11.5	153	13.9	161
KOH-25%	8.9	163	12.1	155	13.3	151
SS-00%	8.2	151	11.9	145	12.1	154
SS-25%	7.1	152	11.1	151	12.3	147
SS-33%	6.4	155	13.1	151	12.0	154
SS-50%	6.5	156	13.2	146	10.5	155

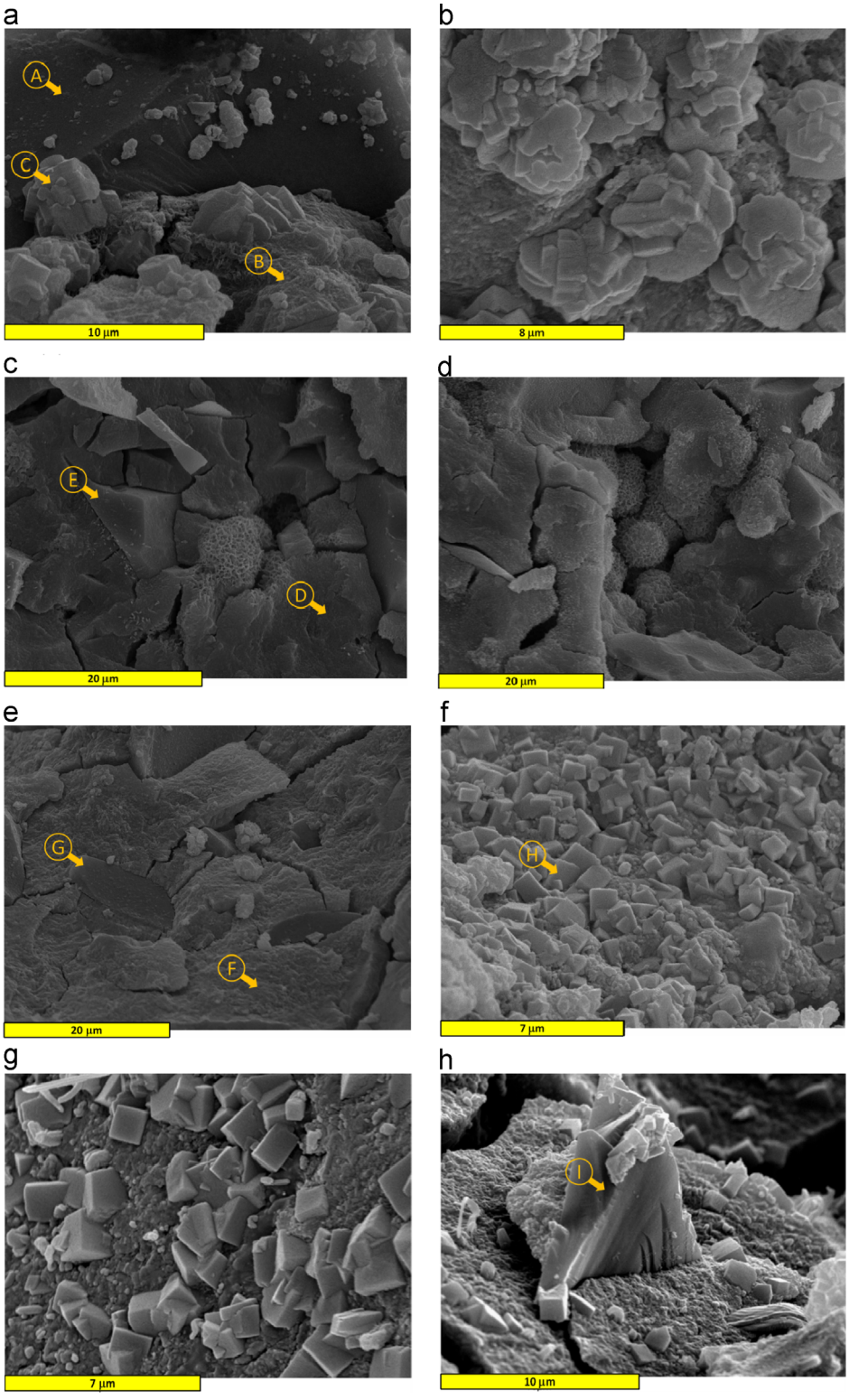

Fig. 7. SEM micrographs of alkali activated pastes 28 days cured (a) NAOH-25% (b) NAOH-25% (c) SS-00% (d) SS-00% (e) KOH-00% (f) KOH-00% (g) KOH-25% (h) KOH-25%.

pozzolans: lower permeability values were found for alkali-activated mortars [33]. In this sense, studies on porosity structure for these new binders must be carried out. Control mortars with BFS (0% SBA) and 25%-replaced SBA mortars were characterised by means of mercury intrusion porosimetry (MIP). Table 6 summarises the most relevant data related to the porosity of studied samples. Total porosity found for samples activated by means of an 8 M NaOH solution was close to 18% (18.17% for NaOH-00% and 17.32% for NaOH-25%), resulting in a reduction in total porosity when SBA was

added. The total porosity for samples activated by means sodium silicate solution (SS) was significantly lower, close to 15%: again, SBA added mortar presented lower total porosity (SS-25%, 14.66%) than control mortar (SS-00%, 15.66%). Mechanical strength data are related to these porosity results, showing that mortars activated using sodium silicate were stronger than NaOH ones. In the case of KOH-activated samples, the total porosity was indeed lower, in part due to the lower water/binder ratio used.

Another interesting behaviour was found for the volume of pores corresponding to capillary network (10–1000 nm range). SS-set and KOH-set mortars showed a low percentage (11–20%) of pores in this pore size range, with this behaviour being very different to that found for the NaOH-set (36–37%). Finally, retained mercury after extrusion step in MIP experiment was determined: again, NaOH-set samples showed the lowest values, finding 54–59% of mercury retention compared to 68–79% for SS-set and KOH-set samples. In general, it can be stated that samples activated by SS or by KOH reagents were better in terms of porosity, and the replacement of BFS by SBA did not produce important changes in the porous structure, revealing the good properties of SBA for alkali-activated BFS systems.

Table 6
Mercury intrusion porosimetry results for mortars cured for 90 days at 25 °C.

Pore size range (nm)	NaOH-00%	NaOH-25%	SS-00%	SS-25%	KOH-00%	KOH-25%
	Volume of pores (%)					
< 10 nm	3.52	2.80	1.51	7.85	2.17	3.23
10 nm $< d <$ 100 nm	19.43	22.69	3.58	12.99	5.39	9.85
100 nm $< d <$ 1 μm	17.33	14.82	8.12	7.97	7.51	8.15
1 μm $< d <$ 10 μm	33.23	34.69	46.65	37.43	41.77	40.49
10 μm $< d <$ 100 μm	11.78	13.03	20.61	15.08	22.49	21.53
$d >$ 100 μm	14.69	12.00	19.59	18.75	20.76	16.79
Total porosity	18.17	17.32	15.66	14.66	11.78	13.58
Median pore diam. (nm)	10.5	15.1	6.9	7.6	8.7	8.7
% Hg retained	58.61	54.56	78.47	68.45	74.16	68.19

Table 7
Water absorption, compressive strength loss (%) and mass loss (%) for mortars submerged in hydrochloric acid (HCl), acetic acid (HAc) and ammonium chloride (NH_4Cl) for 200 days period.

Mortar	Water absorption (%)	Compressive strength loss (%)			Mass loss (%)		
		HCl	HAc	NH_4Cl	HCl	HAc	NH_4Cl
Control	4.4	89.1	94.8	83.3	16.1	12.6	7.0
NaOH-00%	8.3	68.6	58.5	33.4	12.7	6.6	3.1
NaOH-25%	7.4	91.6	62.4	25.7	15.0	6.4	3.1
SS-00%	7.9	85.8	45.6	0.50	14.0	6.9	3.4
SS-25%	7.3	95.3	48.3	12.3	15.6	6.7	3.2
KOH-00%	9.0	89.5	57.4	0.2	13.5	7.3	3.3
KOH-25%	9.9	89.2	73.1	48.4	15.2	7.0	3.9

3.4. Durability studies

Selected alkali-activated mortars from the previous studies were subjected to aggressive solutions, both acid (hydrochloric acid HCl, ammonium chloride NH_4Cl and acetic acid HAc) and sulphate reagents (sodium and magnesium sulphates). The behaviour of these mortars was compared to OPC mortar (cured for 90 days), which had a compressive strength of 52.5 MPa before immersion in aggressive solutions.

Previously, water absorption was measured for mortar samples. Table 7 summarises the obtained values. It can be stated that alkali-activated mortars presented a higher absorption than OPC mortar. This suggests that external attack of

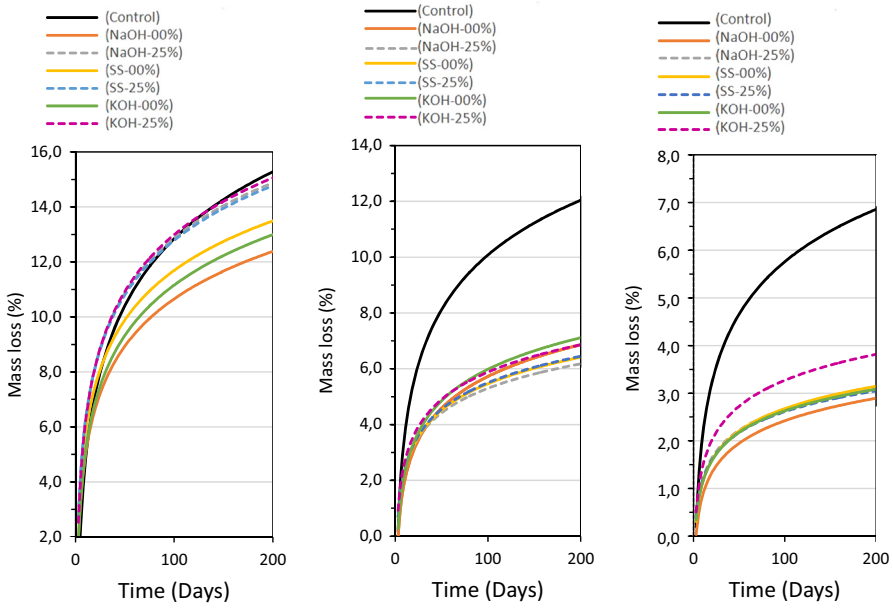

Fig. 8. Mass loss percentage variation for mortar submerged in: (a) hydrochloric acid; (b) acetic acid; (c) ammonium chloride.

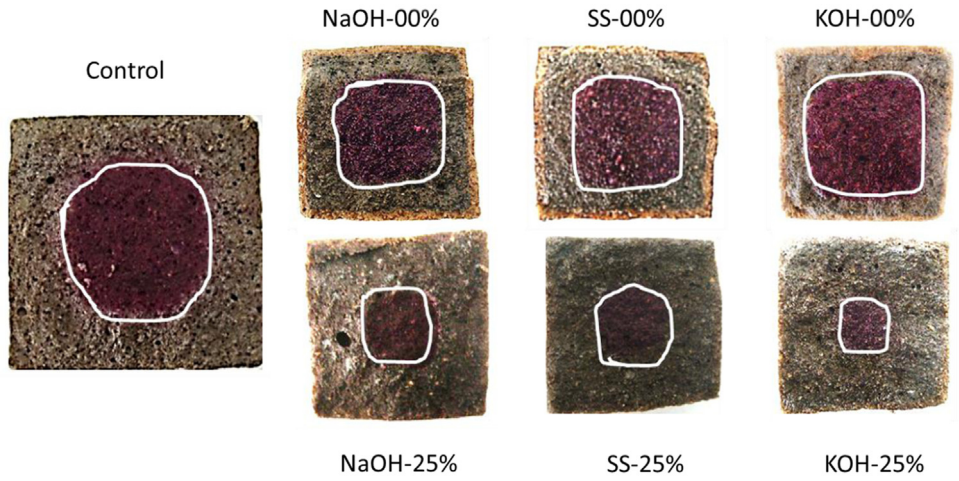

Fig. 9. Phenolphthalein revealed mortars subjected to ammonium chloride solution after 200 days. (For clarity, a solid white line was depicted for delimiting the non-attacked area).

Table 8
Mass loss percentage and compressive strength variation for mortars submerged in sodium (10%) and magnesium (5%) sulphate solutions during 300 days.

Mortar	Variation in compressive strength (%)		Variation in mass loss (%)	
	Na_2SO_4	$MgSO_4$	Na_2SO_4	$MgSO_4$
Control	−64.9	−48.4	4.6	1.7
NaOH-00%	1.6	−8.7	−0.4	1.0
NaOH-25%	−17.2	−28.0	−0.4	2.0
SS-00%	17.2	−37.4	−0.3	2.5
SS -25%	1.2	−48.2	−0.3	3.5
KOH-00%	11.7	−32.1	−0.4	1.3
KOH-25%	0.5	−51.3	−0.9	2.4

alkali-activated mortars would be more pronounced because of accessibility to the internal porous structure.

Table 7 summarises the percentage variation in compressive strength after 200 days of immersion of specimens in the aggressive acid solutions and the variation of mass for different acid media.

In 0.5 M HCl solution, the reduction in the compressive strength was dramatic for all tested mortars and the mass loss was in the 12–16%. Fig. 8a shows the variation of percentage of mass loss for all tested mortars. Control mortar (OPC mortar) and mortars containing BFS/SBA showed similar trends. It is likely that no differences could be observed for this durability test due the combined effect of a long testing period (200 days) and the concentration of HCl. It was expected that alkali-activated binders based on BFS present similar or even superior acid corrosion than Portland cement binders due the absence of portlandite and the low Ca/Si ratio in the alkali-activated binder, a fact that makes these alternative binders more vulnerable to the acid attack [16]. From the presented results, it can be concluded that alkali-activated BFS mortars did not enhance the durability behaviour in HCl 0.5 M, and the partial replacement of BFS by SBA did not change their durability.

In general terms, organic acids such as acetic acid are considered weak and react with hydrated phases of Portland cement (especially portlandite and C–S–H gel), forming calcium salts or complexes. When calcium salts formed due to the attack are soluble, the degradation mechanism can be compared to those produced by strong acids such as nitric and hydrochloric acids [34]. In Table 7, the compressive strength loss (%) and mass loss (%) for an attack of 1 M HAc are summarised. The compressive strength loss for OPC mortar was 94.8%, similar to those found for HCl solutions. Otherwise, for BFS and BFS/SBA alkali-activated mortars, their strength loss values were in the range 45–73%.

Additionally, strength loss percentages for SBA-containing mortars were higher than those for the corresponding BFS mortars (without SBA), suggesting that the mixed matrix (BFS/SBA) was less resistant to acid attack. Mass losses observed for alkali-activated mortars were half of those obtained for OPC. In Fig. 8b, mass loss variations for mortars are depicted. BFS/SBA showed a slightly higher rate of mass respect to BFS mortars.

Finally, for samples immersed in 1 M NH_4Cl medium, a different behaviour was also observed: OPC mortar reduced its strength by more than 90%, whereas in some cases, the reduction in strength for alkali-activated mortars was negligible. The replacement of BFS by SBA produced, in general, mortar with similar durability compared to BFS mortars. In this medium, the mass loss values were the lowest. Interestingly, OPC mortar only had 7% of mass loss but retained only 16.7% of strength, which means that the ammonium cation showed a very intensive leaching effect on the cementing matrix [35]. After mechanical testing, the fracture surface was revealed using a phenolphthalein indicator. Fig. 9 shows some images for all tested mortars after 200 days of NH_4Cl attack. The non-neutralised zone is delimited by a white line. It is noticeable that in OPC samples, an important part of the core specimen was not neutralised, which indicates that the acid did not reach this part. However, the strength was reduced dramatically. For BFS alkali-activated mortars, the

non-neutralised zone is larger, whereas for BFS/SBA alkali-activated mortars, this zone was indeed smaller than those found for OPC. These results enable the following to be stated: on the one hand, despite the neutralising process being important in alkali-activated mortars, no dramatic loss in strength was produced, thus demonstrating the good properties to acid attack of this type of matrix. On the other hand, the replacement of BFS by SBA increased the attacked zone, probably due to the difference in the calcium/magnesium content between BFS and SBA: when SBA is used, the amount of alkaline earth cations in the mixture is reduced, and therefore its ability to delay the attack.

With respect to the behaviour in sulphate media (sodium and magnesium sulphates), strength variation and mass loss variation after 300 days of exposure are summarised in Table 8. OPC mortars expanded severely in both sodium and magnesium sulphate media as expected, and their reduction in compressive strength was very important. A previous paper [36] also showed the expansion and strength loss for alkali-activated pozzolans submerged in a solution of mixed sulphates: 2.5% sodium sulphate and 2.5% magnesium sulphate. Alkali-activated mortars showed a good behaviour in sodium sulphate medium. In general terms, the strength was increased for BFS mortars, whereas a small reduction in strength was observed for BFS/SBA mortars. Finally, the behaviour of alkali-activated mortars in magnesium sulphate solution was not good, being very similar to those found for OPC: large diminution in strength was yielded, indicating that matrices produced by alkaline activation of BFS are not resistant to magnesium attack, and that the addition of SBA did not enhance the behaviour. The obtained results are in accordance with those of Ismail et al. [37], showing that $MgSO_4$ is more aggressive to alkali-activated binders than Na_2SO_4 solution.

4. Conclusions

Sugarcane bagasse is an agricultural waste which can be transformed, for cementing purposes, into an interesting material by auto-combustion. Specifically, the obtained ash (SBA) was successfully used to prepare alkali-activated binders by combining with blast furnace slag (BFS). SBA had a large amount of quartz (by soil contamination); however, it reacted in high alkaline medium. Mixtures of BFS/SBA were used for preparing alkali-activated mortars, by using NaOH, sodium silicate and KOH solutions as activating reagents. The replacement of 25% BFS with SBA generated mortars that yielded similar or higher compressive strength than control mortars (only BFS). Reactivity of SBA was sufficient for compensating the replacement of BFS in these alkali-activated systems. Microstructural studies demonstrated that the hydration products formed in the activation of BFS are not significantly affected by the presence of SBA in the mixture. In terms of durability, alkali-activated mortars exhibit better behaviour than plain OPC mortars, especially in ammonium chloride, acetic acid and sodium sulphate media. In general, the presence of SBA in alkali-activated BFS mortars did not produced significant problems in durability. In conclusion, sugarcane bagasse ash (SBA) obtained by auto-combustion showed good cementing properties as a mineral precursor blended with blast furnace slag (BFS) in alkali-activated systems.

Acknowledgements

The Authors would like to thank the Ministerio de Educación, Cultura y Deporte of Spain (Cooperación Interuniversitaria Program with Brazil, Project PHB-2011-0016-PC), CAPES-Brazil (Project CAPES/DGU No. 266/12), CNPq (Project 401724/2013-1) and Electron Microscopy Service of the Universitat Politècnica de València.

References

[1] A.A. Khan, W. de Jong, P.J. Jansens, H. Spliethoff, Biomass combustion in fluidised boilers: potential problems and remedies, Fuel Process. Technol. 90 (2009) 21–50.
[2] E.M.R. Fairbairn, B.B. Americano, G.C. Cordeiro, T.P. Paula, R.D. Toledo Filho, M.M. Silvoso, Cement replacement by sugar cane bagasse ash: CO_2 emissions reduction and potential for carbon credits, J. Environ. Manag. 91 (2010) 1864–1871.
[3] M. Frías, E. Villar, H. Savastano, Brazilian sugar cane bagasse ashes from cogeneration industry as active pozzolans for cement manufacture, Cem. Concr. Compos. 33 (2011) 490–496.
[4] G.C. Cordeiro, R.D. Toledo Filho, E.M.R. Fairbairn, Effect of calcination temperature on the pozzolanic activity of sugar cane bagasse ash, Constr. Build. Mater. 23 (2009) 3301–3303.
[5] G.C. Cordeiro, R.D. Toledo Filho, L.M. Tavares, E.M.R. Fairbairn, Experimental characterisation of binary and ternary blended-cement concretes containing ultrafine residual rice husk and sugar cane bagasse ashes, Constr. Build. Mater. 29 (2012) 641–646.
[6] M.M. Tashima, J.L. Akasaki, J.L.P. Melges, L. Soriano, J. Monzó, J. Payá, M.V. Borrachero, Alkali activated materials based on fluid catalytic cracking catalyst residue (FCC): influence of SiO_2/Na_2O and H_2O/FCC ratio on mechanical strength and microstructure, Fuel 108 (2013) 833–839.
[7] A. Palomo, P. Krivenko, I. Garcia-Lodeiro, E. Kavalerova, O. Maltseva, A. Fernández-Jiménez., A review on alkaline activation: new analytical perspectives, Mater. Constr. 64 (2014) e022.
[8] M.B. Mohd Salahuddin, M. Norkhairunnisa, F. Mustapha, A review on thermophysical evaluation of alkali-activated geopolymers, Ceram. Int. 41 (2015) 4273–4281.
[9] J. Payá, J. Monzó, M.V. Borrachero, M.M. Tashima, Reuse of alumino-silicate industrial waste materials in the production of alkali-activated concrete binders, in: F. Pacheco-Torgal, J.A. Labrincha, C. Leonelli, A. Palomo, P. Chindaprasirt (Eds.), Handbook of Alkali-Activated Cements, Mortars and Concretes, Woodhead Publishing, Cambridge, 2015, pp. 487–515.
[10] I. Lancelotti, M. Cannio, F. Bollino, M. Catauro, L. Barbieri, C. Leonelli, Geopolymers: an option for the valorisation of incinerator bottom ash derived “end of waste”, Ceram. Int. 41 (2015) 2116–2123.
[11] V.N. Castaldelli, J.L. Akasaki, J.L.P. Melges, M.M. Tashima, L. Soriano, M.V. Borrachero, J. Monzó, J. Payá, Use of slag/Sugar Cane Bagasse Ash (SCBA) blends in the production of alkali-activated materials, Materials 6 (2013) 3018–3127.
[12] V.N. Castaldelli, M.M. Tashima, J.L.P. Melges, J.L. Akasaki, J. Monzó, M.V. Borrachero, L. Soriano, J. Payá, Preliminary studies on the use of sugar cane bagasse ash (SCBA) in the manufacture of alkali activated binders, Key Eng. Mater. 600 (2014) 689–698.
[13] J.S.J. van Deventer, J.L. Provis, P. Duxson, Technical and commercial progress in the adoption of geopolymer cement, Miner. Eng. 29 (2012) 89–104.

[14] B. Singh, G. Ishwarya, M. Gupta, S.K. Bhattachayya, Geopolymer concrete: a review of some recent developments, Constr. Build. Mater. 85 (2015) 78–90.
[15] O. Burciaga-Díaz, J.I. Escalante-García., Strength and durability in acid media of silicate-activated metakaolin geopolymers, J. Am. Ceram. Soc. 95 (2012) 2307–2313.
[16] Z. Bascarevic, The resistance of alkali-activated cement-based binders to chemical attack, in: F. Pacheco-Torgal, J.A. Labrincha, C. Leonelli, A. Palomo, P. Chindaprasirt (Eds.), Handbook of Alkali-Activated Cements, Mortars and Concretes, Woodhead Publishing, Cambridge, 2015, pp. 373–396.
[17] T. Bakharev, j.G. Sanjayan, Y.-B. Cheng, Sulphate attack on alkali-activated slag, Cem. Concr. Res. 32 (2002) 211–216.
[18] T. Bakharev, Durability of geopolymer materials in sodium and magnesium sulphate solutions, Cem. Concr. Res. 35 (2005) 1233–1246.
[19] M.M. Tashima, C.F. Fioriti, J.L. Akasaki, J. Payá, L.C. Sousa, J.L. P. Melges, High reactive rice husk ash (RHA): production method and pozzolanic reactivity, Ambiente Construído 12 (2012) 151–163.
[20] ASSOCIAÇÃO BRASILEIRA DE NORMAS TÉCNICAS – ABNT. NBR 5733: Cimento Portland de alta resistência inicial. Rio de Janeiro, 1991, 5 p.
[21] ASSOCIAÇÃO BRASILEIRA DE NORMAS TÉCNICAS – ABNT. NBRNM 248: Agregados – Determinação da composição granulométrica. Rio de Janeiro, 2003, 6 p.
[22] ASSOCIAÇÃO BRASILEIRA DE NORMAS TÉCNICAS – ABNT. NBRNM 52: Agregado miúdo – Determinação de massa específica e massa específica aparente. Rio de Janeiro, 2009, 6 p.
[23] ASSOCIAÇÃO BRASILEIRA DE NORMAS TÉCNICAS – ABNT. NBR7215: Cimento Portland – Determinação de resistência a compressão. Rio de Janeiro, 1996, 8 p.
[24] ASSOCIAÇÃO BRASILEIRA DE NORMAS TÉCNICAS – ABNT. NBR 9778: Argamassa e concreto endurecidos – Determinação da absorção de água, índice de vazios e massa específica. Rio de Janeiro, 2005, 4 p.
[25] P. Krivenko, G. Kovalchuk, Directed synthesis of alkaline aluminosilicate minerals in a geocement matrix, J. Mater. Sci. 42 (2007) 2944–2952.
[26] X. Liu, H. Sun, X. Feng, N. Zhang, Relationship between the microstructure and reaction performance of aluminosilicate, Int. J. Miner. Metall. Mater. 17 (2010) 108–115.
[27] M.M. Tashima, Producción y caracterización de materiales cementantes a partir del silicoaluminato cálcico vítreo (VCAS) (PhD thesis), Universitat Politècnica de València – UPV (in spanish).
[28] J.E. Oh, P.J.M. Monteiro, S.S. Jun, S. Choi, S.M. Clark., The evolution of strength and crystalline phases for alkali-activated ground blast furnace slag and fly ash-based geopolymers, Cem. Concr. Res. 40 (2010) 189–196.
[29] E. Altan, S.T. Erdogan, Alkali activation of a slag at ambient and elevated temperatures, Cem. Concr. Compos. 34 (2012) 131–139.
[30] B.S. Gebregziabiher, R. Thomas, S. Peethamparan, Very early-age reaction kinetics and microstructural development in alkali-activated slag, Cem. Concr. Compos. 55 (2015) 91–102.
[31] A. Bougara, C. Lynsdale, K. Ezziane, Activation of Algerian slag in mortars, Constr. Build. Mater. 23 (2009) 542–547.
[32] S.A. Bernal, R.M. de Gutiérrez, J.L. Provis, V. Rose, Effect of silicate modulus and metakaolin incorporation on the carbonation of alkali silicate-activated slags, Cem. Concr. Res. 40 (2010) 898–907.
[33] D. Bondar, C.J. Lynsdale, N.B. Milestone, M. Hassani, Oxygen and chloride permeability of alkali-activated natural pozzolan concrete, ACI Mater. J. 109 (2012) 1–10.
[34] S. Larreur-Cayol, A. Bertron, G. Escadeillas, Degradation of cement-based materials by various organic acids in agro-industrial waste-waters, Cem. Concr. Res. 41 (2011) 882–892.
[35] I. Segura, M. Molero, S. Aparicio, J.J. Anaya, A. Moragues, Decalcification of cement mortars: characterisation and modelling, Cem. Concr. Compos. 35 (2013) 136–150.
[36] D. Bondar, C.J. Lynsdale, N.B. Milestone, N. Hassani, Sulphate resistance of alkali activated pozzolans, Int. J. Concr. Struct. Mater. 9 (2014) 145–158.
[37] I. Ismail, S.A. Bernal, J.L. Provis, S. Hamdan, J.S.J. van Deventer, Microstructural changes in alkali activated fly ash/slag geopolymers with sulphate exposure, Mater. Struct. 46 (2013) 361–373.